

Contents lists available at ScienceDirect

Polymer

journal homepage: www.elsevier.com/locate/polymer





Polymers on plasmonic metal nanoparticles: From symmetric coating to asymmetric surface patterning

Hanyi Duan a, Debasmita Muhuri b, Jie He a,b,*

- ^a Polymer Program, Institute of Materials Science, University of Connecticut, Storrs, CT, 06269, USA
- ^b Department of Chemistry, University of Connecticut, Storrs, CT, 06269, USA

ABSTRACT

We summarize recent advances in the design of hybrid nanostructures through the combination of synthetic polymers and plasmonic nanoparticles (NPs). We categorize the synthetic methods of those polymer-coated metal NPs into two main strategies: direct encapsulation and chemical grafting, based on how NPs interact with polymers. In direct encapsulation, NPs with hydrophobic ligands are physically encapsulated into polymer micelles, primarily through hydrophobic interactions. We discuss strategies for controlling the loading numbers and locations of NPs within polymer micelles. On the other hand, polymer-grafted NPs (PGNPs) have synthetic polymers as ligands chemically grafted on NPs. We highlight that polymer ligands can asymmetrically coat metal NPs through hydrophobicity-driven phase segregation using homopolymers, BCPs and blocky random copolymers. This review provides insights into the methodologies and mechanisms to design new nanostructures of polymers and NPs, aiming to enhance the understanding of this rapidly evolving field.

1. Introduction

The past two decades have witnessed remarkable progress in wetchemical synthesis of metal nanoparticles (NPs) in terms of their wellcontrolled sizes, shapes, and chemical composition [1-4]. Those NPs representing atoms and molecules, to some extent, as building blocks to design new functional macroscopical materials through bottom-up approach, have attracted much attention [5-7]. Plasmonic NPs are among the most popular NPs due to their distinctive optical properties originating from localized surface plasmon resonance (LSPR) defined as the coherent oscillation of free electrons under excitation of light at a specific wavelength [8,9]. The electromagnetic field of plasmonic NPs can be amplified when two or more NPs are brought into proximity [10, 11]. Interestingly, the plasmonic coupling of NPs can result in collective properties such as new plasmonic model not existing in discrete NPs [12, 13]. When coupled at a distance smaller than their particle sizes, the enhanced electromagnetic field in between NPs induces a strong local dipole change of molecules that further enhances their Raman scattering [14,15]. This concept has been broadly used for sensing and detection in surface enhanced Raman spectroscopy (SERS) [16-20]. While the controllable self-assembly of plasmonic NPs in solution provides a paradigm to utilize their plasmonic features, how to program their assemblies and achieve desired ensemble properties remains as an unmet challenge.

Adding polymer as surface ligands to NPs or encapsulating NPs into polymers offers such a possible solution to tailor their assemblies [21 – 23]. Synthetic polymers can control the interparticle interaction and thus guide how metal NPs self-assemble [24 - 26]. Using polymers as surface ligands for NPs is advantageous. First of all, as-synthesized colloidal NPs are usually capped by molecular ligands (or capping ligands) and they are stabilized by either electrostatic repulsion in aqueous solution or weak steric interaction in organic solvents [27 - 29]. Those colloidal NPs can be easily destabilized by ionic strength or other competitive binding species like thiols, amines or acids [30 - 33]. Grafting polymers on NPs provides a large steric repulsion, because the size of polymer is often comparable to that of NPs. The polymer layer as a nanometer "buffer" helps overcome van der Waals attraction between NPs to provide stable solvation and improve their long-term colloidal stability. The polymer layer can also prevent the atomic dissolution from metallic cores, as their chemical buffer zooms against strong acids or oxidants. Secondly, polymers can stabilize NP assemblies. In a kinetically controlled process (most of NP assemblies are kinetic products), polymers effectively freeze the assembled structures and prevent their irreversible precipitation or reversible dissociation [34]. This is extremely important for electron microscopic characterization of NP assemblies where those assembled nanostructures are kinetically frozen during solvent removal. Third, polymers may create nanostructures on the surface of NPs under specific conditions and generate NPs with

 $^{^{\}mbox{\tiny $\dot{\tau}$}}$ Celebrating the 70th Anniversary of the Polymer Program at Sichuan University.

^{*} Corresponding author. University of Connecticut, Storrs, CT, 06269, USA. E-mail address: jie.he@uconn.edu (J. He).

Polymer 303 (2024) 127115

unique structural asymmetry as reported recently [35-38]. Such topological features provide directional interactions that are of key importance for their controllable self-assembly in terms of both direction and strength. These characteristics through the coupling of NPs and polymer are often missing in their pristine or capping ligand counterparts.

There are different ways to hybridize polymers and NPs. In the current review, we will categorize them as physical adsorption (polymers have no covalent interaction with NPs) and chemical grafting (polymers are chemically bound to NPs). In physical adsorption, hydrophobic molecular ligands are usually used to first modify the surface of NPs. Synthetic polymers like amphiphilic block copolymers (BCPs) are further added together with water to trigger the physical encapsulation of NPs. The hydrophobic interaction between NPs and polymers drives such physical adsorption of polymers onto clusters or other aggregates of NPs. On the other hand, chemical grafting usually involves polymers having one or more binding motif(s) to NPs. Polymers are grafted "from" or "to" NPs covalently, also termed as polymer-grafted NPs (PGNPs). As surface ligands, polymers that dominate the interparticle interaction can drive the self-assembly of PGNPs. To simplify the discussion, we will summarize our review based on how polymers interact with NPs. We will first introduce the encapsulation of NPs with molecular ligands in synthetic polymer mediated by hydrophobic interaction, with a focus on symmetric/asymmetric surface coating and NP clustering in polymer domains. In the second part, we will cover the polymer-guided self-assembly of PGNPs in solution. Patchy NPs with precisely controllable topological structures will be highlighted with new synthetic strategies such as phase separation of mixing ligands and hydrophobicity driven surface dewetting. Those polymer-induced

surface asymmetry of NPs will be discussed as building blocks for polymer-guided self-assembly. Overall, we interpret the methodology and mechanistic insights with our own understanding on polymer ligand chemistry of NPs, which we think would be helpful for readers to fundamentally appreciate the forefront of the topic.

2. Surface coating of polymers on NPs guided by small molecule ligands

Ligands play a crucial role in dispersing colloidal NPs in solution to prevent their aggregation. Hydrophobicity/hydrophilicity of NPs is solely dominated by their surface ligands. While NPs capped with hydrophobic ligands are not stable in aqueous solution, they can be encapsulated in hydrophobic cores of polymer micelles. Amphiphilic diblock BCPs as an example can self-assemble into core-shell nanostructures with a hydrophobic core and a hydrophilic corona upon adding a selective solvent like water. In the presence of NPs capped with hydrophobic molecular ligands, hydrophobicity can drive physical encapsulation of NPs into polymer micelles, also known as co-selfassembly. Taton's group pioneered the co-self-assembly of metal NPs and amphiphilic BCPs [39]. The co-self-assembly can be carried out by mixing citrate-capped gold NPs (AuNPs) with a small amount of n-dodecanethiol (DT) and amphiphilic polystyrene-block-poly (acrylic acid) (PS100-b-PAA13) in DMF. DT would quickly modify AuNPs to generate a hydrophobic surface. Upon the addition of water, hydrophobic AuNPs became thermodynamically unstable in the solvent mixture, and they could be physically encapsulated by the hydrophobic PS core of PS₁₀₀-b-PAA₁₃. Those hybrid core-shell nanostructures were

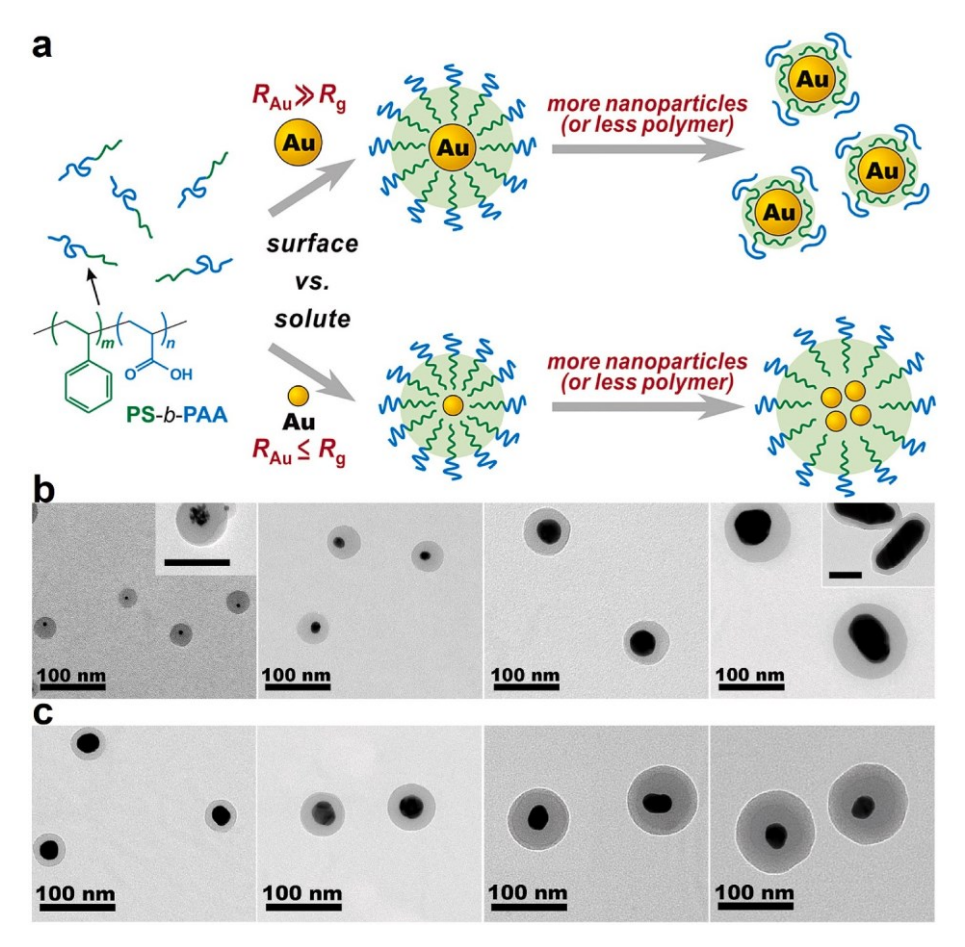


Fig. 1. (a) Scheme showing the impact of R_{Au}/R_g ratio on the number of NP inside polymer micelles. (b) TEM images showing the size effect of AuNPs encapsulated by PS_{100} -b-PAA₁₃ (0.1 mg/mL) (from left to right: $d_{Au} = 4.1$, 12.3, 30.0 and 52.4 nm). (c) TEM images showing the effect of relative AuNP surface area on the polymer shell thickness (from left to right: $[PS_{100}$ -b-PAA₁₃]/nA_{Au} = 2.6, 13, 65 and 325). Reprinted with permission from Ref. [39]. Copyright 2005 American Chemical Society.

stabilized by hydrophilic PAA corona. The number of AuNPs inside the PS core was dependent on the relative size of AuNPs and the chain length of PS, defined as the ratio of $d_{\text{Au}}\!/R_{\text{g}}$ (d_{Au} is the diameter of AuNPs and R_{g} is the radius of gyration of the PS block, Fig. 1a). With $d_{Au}/R_g \approx 1$ ($d_{Au} =$ 4.1 nm), the clusters of multiple AuNPs with each polymer micelle were observed. In the case of $d_{Au}/R_g > 1$ ($d_{Au} = 12.3, 30.0$ and 52.4 nm), core-shell NPs with discrete AuNPs in each micelle were found (Fig. 1b). The shell thickness was also tunable by adjusting the relative ratio of polymer concentration to the total surface area of AuNPs ([PS $_{100}$ -b-PAA $_{13}$]/A $_{Au}$). Increasing the BCP concentration or decreasing the AuNP concentration (proportional to the surface area of AuNPs) effectively increased the shell thickness from 9 nm to 40 nm without changing the number of AuNPs encapsulated as shown in Fig. 1c. The PS shell thickness can be further controlled by BCP, where a longer PS block length (N) resulted in a thicker polymer shell under the same concentration. The scaling law was described as $l_{\rm shell} \propto N^{0.33}$. Later, the same group also demonstrated that AuNPs encapsulated within the core-shell structures exhibit a red-shifted plasmon resonance and prevent the cyanide etching due to the existence of the hydrophobic PS shell [40].

The early examples from the Taton group provide the key roadmap of the co-self-assembly strategy to design hybrid core-shell nanostructures with exquisite shell thickness control, although it is highly desirable to precisely control the number of NPs inside the polymer micelle to obtain core-shell structure with exactly two, three, or multiple NPs. For plasmonic NPs, the number of NPs is of key importance to control their interparticle plasmon coupling. In terms of the precise number of NPs in each core-shell nanostructure, kinetic control became more important. However, hydrophobicity-driven self-assembly of NPs, in the absence of amphiphilic BCPs, is a continuous process where the number of NP clusters will continuously increase till precipitating out from solution [41]. Amphiphilic BCPs as surfactants can encapsulate NP clusters at any given stage of self-assembly to control the average number of NPs in each nano-assembly. The number in NP clusters would always be polydisperse.

To get the precise number of NPs in each cluster, a density-gradient separation is needed. That is, after triggering the co-assembly of NPs and polymers, separating aggregates containing different numbers of NPs will be carried out. Chen et al. reported the preparation of AuNP dimers and trimers in the core-shell structures by density-gradient centrifugation (Fig. 2a) [34]. With 15 nm AuNPs modified by 2-naphthalenethiol, the clustering of AuNPs was first triggered by adding NaCl in a mixture

of DMF and water induce the random aggregation of AuNPs. Afterwards, PS₁₅₄-b-PAA₆₀ was introduced to encapsulate those aggregates in the early stage, leading to a mixture of hybrid core-shell NPs with 71 % of single AuNP, 24 % of dimers, 5 % of trimers and 0.5 % of tetramers before purification. Those clusters with different numbers of AuNPs had different density and they could be separated by density-gradient centrifugation in a concentrated CsCl solution (11 % top layer + 62 % bottom layer). Two distinct color bands of red and yellow were generated after the first-time centrifugation, corresponding to discrete AuNPs and dimers, respectively. The separated dimers had a purify of 85 % as examined by TEM and it could be further boosted to 95.1 % after a second time centrifugation. After most of individual AuNPs and dimers were extracted, trimers could be isolated with a purify of 81 % by applying the same method to a pre-enriched solution, which gave a blue band after centrifugation. Purified clusters showed distinct color resulting from their surface plasmon coupling. The longitudinal LSPR bands located at 600 nm and 610 nm were observed, corresponding to dimers and trimers of AuNPs, respectively. The hotspots generated by interparticle coupling between dimers or trimers can be further used for SERS [42]. Similar synthetic strategy can be used for Au - Ag core-shell NPs (20 nm) to prepare pure dimer (85 %) and trimers (70 %) of those bimetallic NPs (Fig. 2b). The reason for the choice of core-shell Au - Ag is due to the higher SERS sensitivity of Ag. The averaged SERS intensity for dimers and trimers was 16 and 87 times higher than that on discrete NPs, respectively, due to the enhanced plasmon field in between those NP clusters. The assembly-encapsulation-separation method as a powerful tool to control nanoclusters with high purity also enables the study of their plasmon coupling in NP clusters with different packing geometry [43].

Those clusters of dimers and trimers often consist of NPs with identical sizes and shapes. To mimic the complexity of chemical bonds, NP building blocks can further be tailored with different sizes or chemical identities. The same group demonstrated the stoichiometric control over the assembly of NP clusters [44]. The two AuNP building blocks with same size (d = 18 nm), namely A- and B $^-$ NP, capped by tetrathiol and citrate, respectively. The A-NP with excess of thiols on the surface was capable of binding B-NP. When treating A-NP with excessive B-NP (A/B = 1/16), A-B clusters formed; then, those dimeric clusters were encapsulated by PS-b-PAA. The stoichiometry of A-B clusters could be controlled by balancing the charge repulsion and van der Waals interaction. With continuously decreasing the ionic strength of the

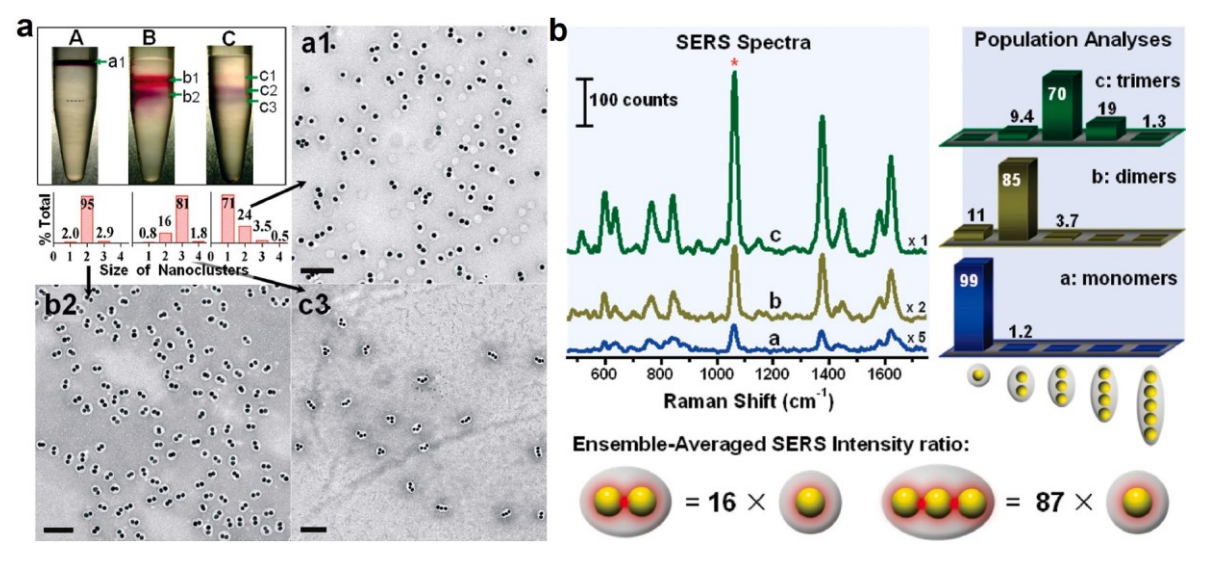


Fig. 2. (a) NP clusters purification by gradient centrifugation. Sample A: NP cluster solution was layered on the top of CsCl aqueous solution; Sample B: A after 20 min centrifugation; Sample C: separation of a pre-enriched trimer solution. TEM images for a1, b2, and c3 represent purified monomer, dimer and trimer encapsulated by PS₁₅₄-b-PAA₆₀, respectively. Reprinted with permission from Ref. [34]. Copyright 2009 American Chemical Society. (b) SERS spectra of 2-naphthalenethiol obtained in purified Au – Ag NP monomer, dimer, and trimer encapsules. Reprinted with permission from Ref. [42]. Copyright 2010 American Chemical Society.

solution, AB_2 -type clusters could be formed with a yield of 89.4 % after purification. The charge repulsion between B-NP could be further compromised with salt. AB_3 -and AB_4 -type clusters were also synthesized with a yield of 65.6 % and 64.9 %, respectively.

Homogeneous surface grafting with hydrophobic molecular ligands usually leads to the concentric encapsulation of NPs or NP clusters into polymer micelles where the conformational entropy of polymer chains is minimum. Thus, it is thermodynamically not possible to tune the location of NPs inside polymer micelles by merely changing the concentration of BCPs and molecular ligands. Breaking the surface homogeneity of NPs by simply introducing another hydrophilic ligand can impact how NPs would interact with polymer micelles. Park and her group demonstrated the control of NP distribution in polymer micelles by tuning the surface hydrophobicity of NPs [45]. Two thiol ligands namely n-dodecanethiol (DT) and mercaptoundecanol (MUL) were used to modify AuNPs (radius ~2.5 nm) as hydrophobic and hydrophilic ligands, respectively. Those AuNPs with mixed ligands could co-self-assemble with PS250-b-PAA14 in DMF and water, subsequently followed by dialysis against water to freeze their assemblies. Due to their small sizes, AuNPs tended to form clusters during encapsulation. With 100 % DT, AuNPs segregated into clusters at the center of the PS core (Fig. 3b). When increasing the mole fraction of hydrophilic MUA, AuNP clusters gradually moved to the interface of PS and PAA forming symmetry-breaking Janus-type nanostructures (Fig. 3c). With the mole fraction of MUA over 50 %, amphiphilic AuNPs uniformly resided at the interface of PS and PAA as surface decors shown under transmission electron microscopy (TEM, Fig. 3d). The calculation suggested that the interfacial energy between the two polymer blocks (PS and PAA) and AuNPs would be minimized at 60 - 100 % of MUL surface coating relative to DT, consistent with experimental observation. Interestingly, with 100 % MUL surface coverage, AuNPs could decorate the surface of preformed polymer colloidal structures like 1-D rod-like micelles or commercial PS-COOH beads, affording various nanocomposites that would be difficult to prepare using simultaneous co-self-assemble method (Fig. 3e - g). Such strategy is also capable of producing assemblies with multiple components such as layered structures with iron oxide NPs arranged in between PS core and AuNPs located at the PS-PAA interface. The same group has applied this method to polymersomes, where

polymer vesicles uniformly decorated with NPs were fabricated through the interfacial co-self-assembly of MUL-capped AuNPs (2.3 nm) and amphiphilic BCPs (PS-b-PAA or PEO-b-PLA) [46].

With larger AuNPs ($d_{Au}/R_g > 1$), it is also possible to control the distribution of individual NPs in polymer micelles. Chen's group demonstrated a "mix-and-heat" method to synthesize Janus-type NPs using 15 nm AuNPs capped by a mixture of hydrophobic/hydrophilic ligands (Fig. 4a) [47]. This method relied on the binding competition of hydrophobic/hydrophilic ligands and subsequent ligand separation on the surface of NPs. A hydrophobic molecular thiol with a long alkyl tail (C15) was used as LA, whereas diethylamine or 4-mercaptobenzoic acid was used as hydrophilic ligands, labelled as L_B. Such mixed ligands were grafted on AuNPs while annealing in the presence of PS₁₅₀-b-PAA₆₀. When the ratio of L_A/L_B varied from 1/0 to 1/22 and 1/132, AuNPs moved from the center of polymer micelles to the surface where the nanostructures evolved from core-shell to slightly eccentric and finally high eccentric (Fig. 4b - g). The increase of the L_B/L_A ratio would lead to more exposed surface of AuNPs. Such an eccentric encapsulation of NPs was considered under a near-equilibrium condition as revealed by the fact that the ligand association/dissociation and separation directly resulted from the balance of surface hydrophilicity/hydrophobicity.

Symmetry-breaking encapsulation has also been achieved on anisotropic NPs like 2-D nanoprism (NPr). Anisotropic NPs have different surface facets originating from their asymmetrical structural features which further allow selective ligand absorption under specific conditions [25,49 - 51]. Such selective ligand grafting may come from surface atoms with low coordination numbers, e.g., edge, corner, or tip sites with higher surface energy and loosely packed capping agents. Chen et al. reported that amphiphilic BCPs could selectively patch tip and/or edge sites of AuNPrs (length of 59 nm and thickness of 21 nm) induced by the selective grafting of ligand islands (Fig. 4h) [48]. AuNPrs were first mixed with 2-naphthalenethiols (2-NAT) as ligands and PS₄₉-b-PAA₁₅₄ as the BCP surfactant in DMF and water (82:18, vol), followed by thermal annealing at 110 °C for 2 h. After purification, patchy AuNPr with three polymer nanospheres functionalized at tips were received at $C_{2-NAT} = 0.12 \mu M$. The selective polymer coverage was attributed to the presence of 2-NAT at tips and the subsequent BCP adsorption driven by hydrophobic interaction. The polymer nanospheres were uniform with a

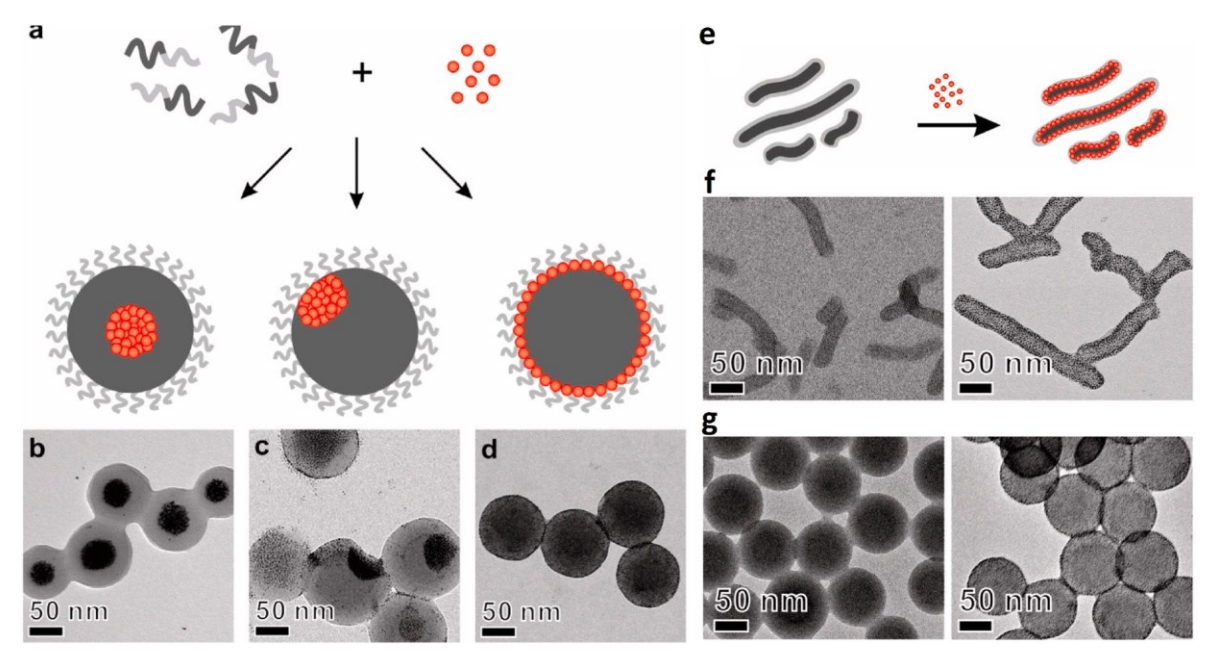


Fig. 3. (a) Schematics to show the different location of NPs in polymer micelles. (b - d) TEM images showing NP clusters located at the center, edge and interface of polymer micelles, respectively. (e) Schemes showing the rod-like micelle decorated with AuNPs. (f) TEM images of rod-like micelles before (left) and after (right) AuNPs decoration. (g) TEM images of PS beads before (left) and after (right) AuNPs decoration. Reprinted with permission from Ref. [45]. Copyright 2013 American Chemical Society.

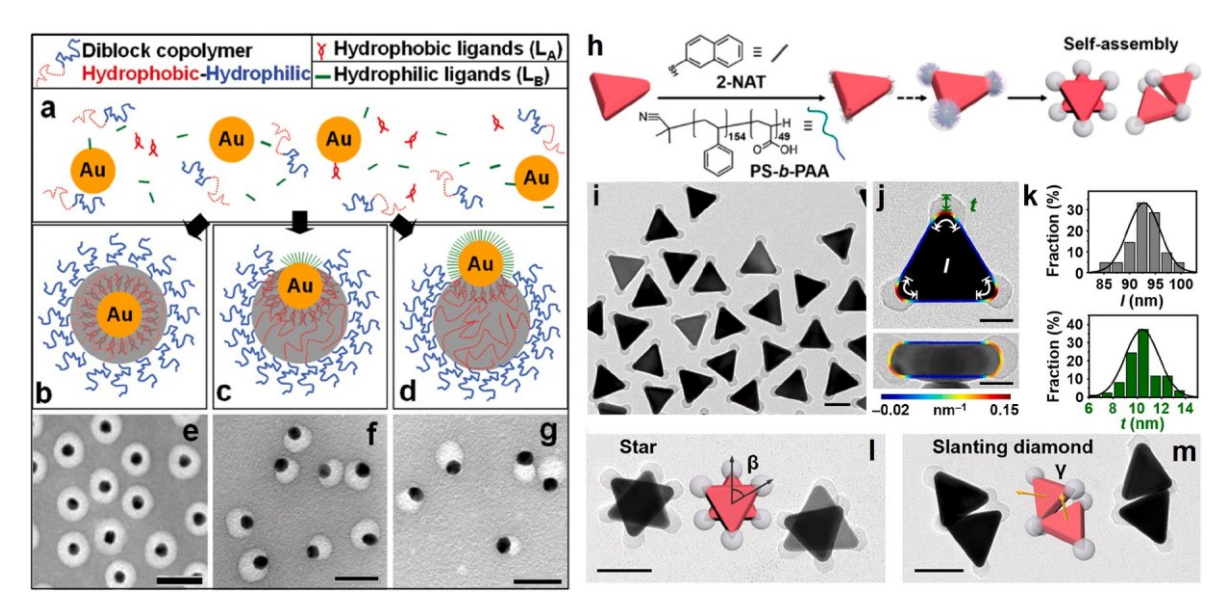


Fig. 4. (a – d) Scheme to show the formation of concentric (b) and eccentric (c and d) AuNP-polymer nanostructures by small molecular ligand phase separation followed by subsequent BCP adsorption. (e, f and g) TEM images of purified AuNP coated by polymer at ligand ratio (L_A:L_B) of 1:0 (e), 1:22 (f) and 1:132 (g). Reprinted with permission from Ref. [47]. Copyright 2008 American Chemical Society. (h) Scheme showing the preparation and self-assembly of patchy AuNPrs. (i) Low magnification TEM image of tip patched AuNPrs. (j) TEM images of tip patched AuNPrs at two different view directions. (k) Histograms of the cover length l and patch thickness t of the patchy AuNPrs. (l and m) TEM images and schematics showing the star and slanting diamond assemblies. Reprinted with permission from Ref. [48]. Copyright 2019 American Chemical Society.

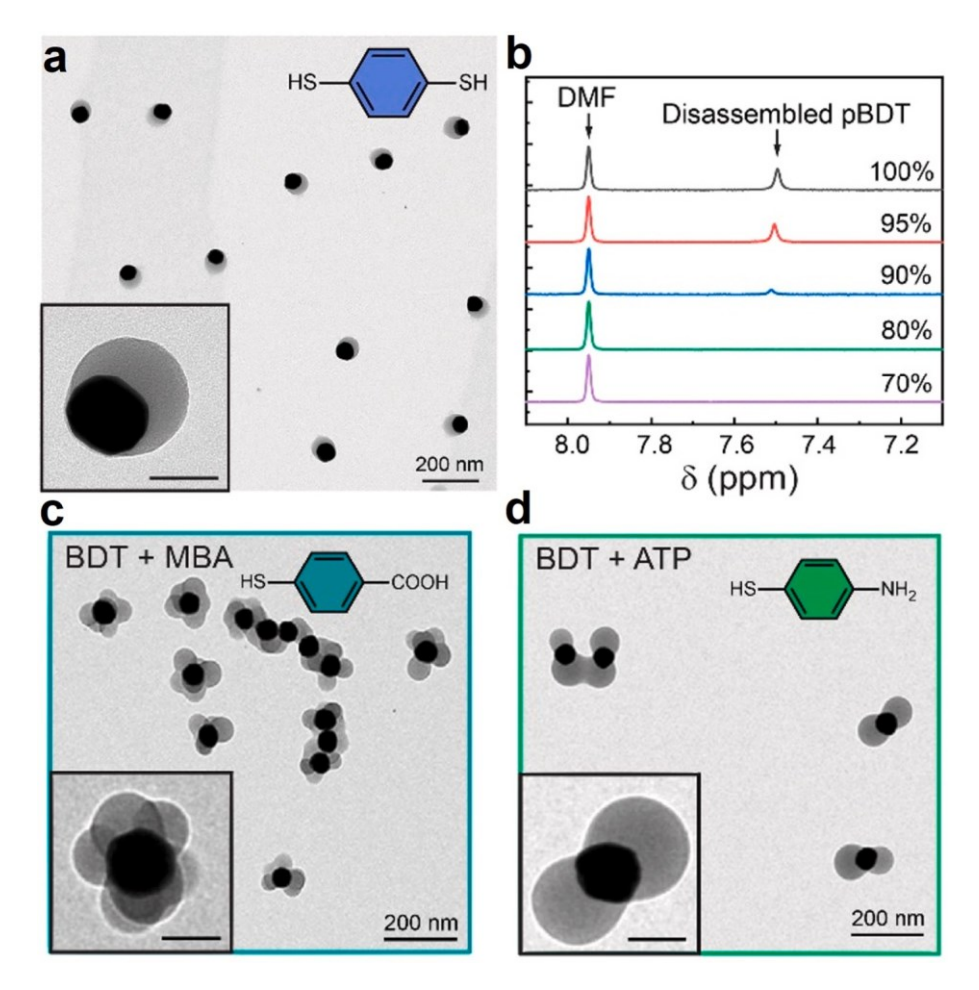


Fig. 5. (a) TEM image showing the Janus AuNP obtained by the self-polymerization of BDT. (b) NMR spectra of Janus AuNP in mixture of D₂O and DMSO-*d*₆ with different volume ratio (Bottom to top: DMSO-*d*₆ vol% increased from 70 % to 100 %). (c and d) TEM images of patchy AuNPs with different morphology obtained by the addition of a second thiol. Reprinted with permission from Ref. [53]. Copyright 2021 American Chemical Society.

low dispersity in the cover length of the patch along the prism contour and shell thickness, ca. 4 % and 13.5 %, respectively. When continuously increasing C_{2-NAT} from 0.12 to 2.5 μ M, polymer nanospheres evolved to trefoil, T-shaped and eventually reuleaux triangle that covered the entire edge sites of AuNPrs. The thickness of polymer domains was tunable by changing the BCP concentration. Tip-patched AuNPr could serve as building blocks for directional self-assembly (Fig. 4l and m). When increasing the ionic strength to screen the electrostatic repulsion of patchy AuNPrs, they self-assembled into stars and slanting diamond nanostructures, where nanoprisms were arranged in face-to-face and side-by-side, respectively. Recently, the same group demonstrated the preparation of AuNPrs with asymmetric polymer patches by utilizing the polymer-polymer attraction to control the number of tip patches on AuNPrs [52]. They proposed that the existing polymer at tips would attract free polymer chains in solution and break the adsorption symmetry at specific conditions due to more favorable chain-chain interaction. Such theoretic interpretation was validated by the fact that the increase of annealing temperature or 2-NAT concentration would lead to the decrease in the yield of patchy AuNPrs with symmetry-breaking polymer nanospheres. Specifically, single patched AuNPrs with a yield as high as 82 % could be obtained at 90 °C and $C_{2-NAT} = 25$ nM. Those nanostructures could further self-assemble into nano-bowtie by patch

More recently, Jesse et al. demonstrated a distinct strategy to prepare patchy nanostructures with molecular ligands through in situ polymerization [53]. 60 nm AuNPs were mixed with benzene-1,4-dithiol (BDT, Fig. 5a) in a buffer solution. Those dithiols could not only modify the surface of AuNPs chemically, but also undergo self-polymerization by forming disulfide bridges. The polymerized BDT chains (pBDT) had a hydrophobic backbone which could progressively assemble onto the surface of NPs covered by pre-adsorbed BDT and led to the formation of polymer patches (~40 nm) (Fig. 5b). The patch size was controllable by the BDT concentration. The introduction of a second monothiol had a great impact on the patch morphology (Fig. 5c and d), where a dimer or octahedral conformation of patches was seen with 4-aminothiophenol (ATP) or 4-mercaptobenzoic acid (MBA). When nonthiol aromatic dye was added together with BDT, the location of Au core relative to the patch could be adjusted from eccentric (fluorescein sodium) to concentric (rhodamine B and azure A chloride).

3. Asymmetric surface patterning induced by polymer ligands

Using polymer ligands to functionalize NPs has received numerous interests in the past decade. The long backbone of polymer ligands makes it possible to rationally integrate hydrophilicity/hydrophobicity and incorporate diverse chemistry/functional groups to the hybrid nanostructures, as compared to small molecules. Polymer ligands have a binding motif (e.g., thiols and carbenes) to link a long polymer backbone to NP cores. For noble metal NPs, thiol has been used as the binding motif in most of reported PGNPs due to its synthetic versatility and moderate binding strength, although some other ligands like N-heterocyclic carbene (NHC) are also documented recently [54,55]. When adding polymers on the surface of NPs, the hydrophobicity or amphiphilicity was often utilized to drive the self-assembly of PGNPs. For example, Zubarev et al. demonstrated the amphiphilicity-driven self-assembly of AuNPs grafted by V-shaped BCPs [56]. Kumacheva's group reported the self-assembly of ABA triblocky gold nanorods (AuNRs) tethered with PS [25]. Later, amphiphilic BCP ligands like PS-b-PEO-SH or mixed polymer brushes have been reported to drive the self-assembly of metal NPs as clusters, vesicles, or tubules in water [57 - 59]. Furthermore, the encapsulation of PGNPs in cylindrical polymer micelles through templating by supramolecular block copolymer self-assembly was also demonstrated by Zhu's group [60,61]. Those self-assembly nanostructures of PGNPs in various assemblies have been summarized in our recent review paper [21,62]; thus, we will not discuss them here in detail. Instead, we will focus on the use of polymer

ligands to asymmetrically coat metal NPs with an emphasis on hydrophobicity-driven surface dewetting.

In 2016, Kumacheva's group has conceptualized a surface patterning method using hydrophobicity-driven phase segregation of PS on the surface of AuNPs [63]. Cetrimonium bromide (CTAB)-capped AuNPs with different size (20 - 60 nm) were modified by thiol-terminated polystyrene (PS-SH, 29 - 50 kDa) in DMF, to which water (4 vol%, very close to its critical water concentration) was introduced to trigger the collapse of PS chains. While PS ligands may graft on AuNPs randomly, the PS shell could evolve from core-shell uniform coating to asymmetric patches, by changing its surface grafting density (Fig. 6a). The patch formation and morphology were dependent on the NP diameter (D), PS ligand length (R, chain radius) and grafting density (O). PS domains segregated as patches at a low σ or on small NP. When keeping σ and D as constant, the decrease of the ratio of R/D would increase the patch number per NP. As an example, 20 nm AuNP with 50 kDa PS-SH at a grafting density of 0.03 chain/nm² gave single patch NP with a yield of 98 %. When D increased to 34 nm, the yield of NPs with single patch and two patches were 34 % and 53 %, respectively. Those trends could be explained by considering the balance of polymer-solvent interfacial energy and the energy cost for stretching end-tethered PS. Hydrophobicity-driven phase segregation of polymer ligands provided new insights into patterning NPs with defined polymer domains. However, those PS-patched AuNPs were not water-soluble. The concentration window of water to trigger the formation of patches was very narrow in order to maintain the colloidal stability of NP. In addition, the NP concentration need to be relatively low to avoid random aggregation. Those drawbacks limited the application of this method for scalable syntheses of polymer-patched NPs. To overcome those challenges, other studies have shown the use of amphiphilic BCPs or random copolymers to drive surface dewetting strategies for scalable syntheses, where those polymer-patched NPs can be dispersed in water [37,64,65].

Using the blocky random copolymers of PEO₄₅-b-P (AA $_{\alpha}$ -r-St_{1- α})_y-b-PSt_x-SH, with α , x, and y variables representing the number of repeating units in each block, respectively, Nie and co-workers have demonstrate water-soluble polymer-patched AuNPs [37]. PEO₄₅-b-P (AA $_{\alpha}$ -r-St_{1- α})_y-b-PSt_x-SH could graft on AuNPs (35.8 nm) through dynamic detachment/attachment upon thermal annealing (Fig. 6b). When the thermal annealing reached a temperature above the upper critical solution temperature in a DMF/water mixture, polymer ligands became

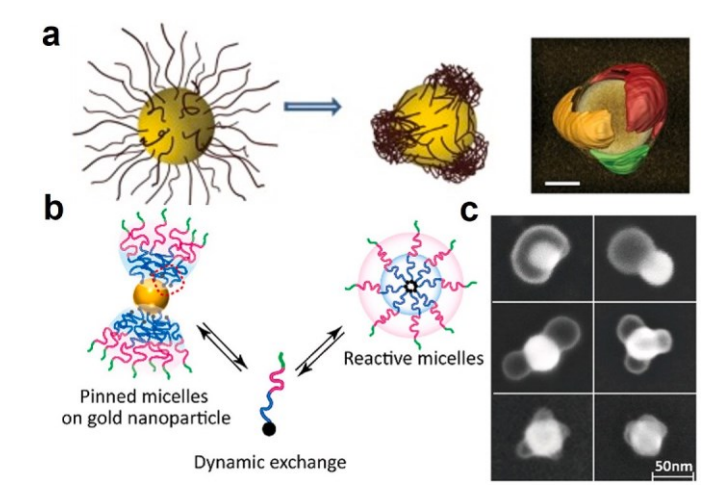


Fig. 6. (a) Schemes to show the formation of a three patched AuNP driven by hydrophobicity and its electron tomographic reconstruction image. Adapted with permission from Ref. [63]. Copyright 2016, Nature Publishing Group. (b) Schemes to show the dynamic ligand exchange between the polymer grafted AuNP and free micelle. (c) SEM images of patchy AuNPs with different morphologies. Reprinted with permission from Ref. [37]. Copyright 2021 American Chemical Society.

very dynamic to exchange with free polymer micelles. This dynamic detachment/attachment controlled the equilibrium distribution of polymer ligands on AuNPs, likely through oxidative elimination and reductive addition as proposed by Liu et al. [66] The change in water content and the volume fraction of the PS block, f = x/(x + y), could tune the number of polymer domains, e.g., 1 - 6 patches per AuNPs (Fig. 6c). For example, with 10 or 20 vol% of H₂O, one or two patches per AuNPs were formed with a yield of 97.5 % and 85 %, respectively, using $PEO_{45}\text{-b-P}\ (AA_{0.3}\text{-}r\text{-}St_{0.7})_{200}\text{-b-PSt}_{633}\text{-SH}$ as ligands. With a constant water content of 20 vol%, a decrease in the hydrophobic fraction (f) from 0.76 to 0.49 (P $(AA_{0.3}-r-St_{0.7})_{200}$ -b-PSt₂₇₀) or 0.39 (P (AA_{0.3}-r-St_{0.7})₂₀₀-b-PSt₁₇₅) would generate AuNPs with three patches or four patches, respectively. At f = 0.49, lowering the H_2O content to 5 vol % would afford open-configuration patch. Therefore, the number of polymer patches on AuNPs could be lowered through either increasing water content or decreasing the fraction of the PS block within the blocky random copolymer. The formation of polymer patches was a result of the dynamic binding of copolymer brushes and the molecular exchange between free polymer micelles and grafted AuNPs. As revealed by TGA results, at elevated temperatures the grafting density gradually decreased from 0.047 to 0.019 chains/nm² due to the labile Au - S bonds and the increase of polymer solubility.

Recently, our group reported the preparation of Janus-type patchy NPs through one-step hydrophobicity-driven surface dewetting with a BCP surfactant [35]. Asymmetric patterning of spherical AuNPs could be achieved by lowering the concentration of polymer ligands where they would dewet the surface of AuNPs at a critical low ligand density driven by the minimization of interfacial energy between polymers and solvents. Citrate-capped AuNPs (13.1 nm) were first mixed with PS₂₀₀-SH (0.9 μ M) as hydrophobic ligands and PS₅₅-b-PAA₁₀₇ (73.5 μ M) as an

amphiphilic BCP surfactant in DMF. Afterwards, 15 vol% of water was introduced to the DMF solution and the mixture was then annealed at 100 °C for 1 h. The final products were quenched in excess water and purified to remove free polymers. TEM characterization revealed snowman-like structures where one micelle-like patch (d = 29.6 nm) on the surface of each AuNP were formed with a yield of 91 % (Fig. 7a). The polymer patch was composed of PS ligands and the PS block from the BCP, whereas the PAA block served as a corona to stabilize those hybrid structures. The concentration of PS₂₀₀-SH was founded to play a key role in the morphology of patchy NPs. When the concentration of PS₂₀₀-SH was in the range of 20.3 to 0.5 μ M, clear morphological transitions from nanoclusters to core-shell NPs, and eventually to Janus NPs were observed. The mechanism behind this dewetting phenomenon is that the decrease in the concentration of PS₂₀₀-SH as a Langmuir adsorption model enabled precise control over surface grafting. At a high grafting density, PS ligands were stretched and the phase segregation did not happen due to steric repulsion of polymer ligands. However, at a low grafting density with relaxed PS chains, the surface dewetting was observed to minimize the interface of polymers and solvents. In the presence of BCPs, the segregated PS domains were further covered and stabilized by BCPs. The obtained Janus type patch NPs had excellent colloidal stability in water due to the presence of hydrophilic PAA and those NPs could be stored in a high concentration for several months. Compared to the binary mixed ligands and solely BCP ligands, this method showed robustness in terms of simplicity and ligand accessibility.

We explored the self-assembly of these patchy AuNPs through directional interactions provided by their surface asymmetry [36]. The seed-mediated growth was employed to grow the Au core from 14 nm to up to 40 nm while retaining the polymer patch size, as a means to

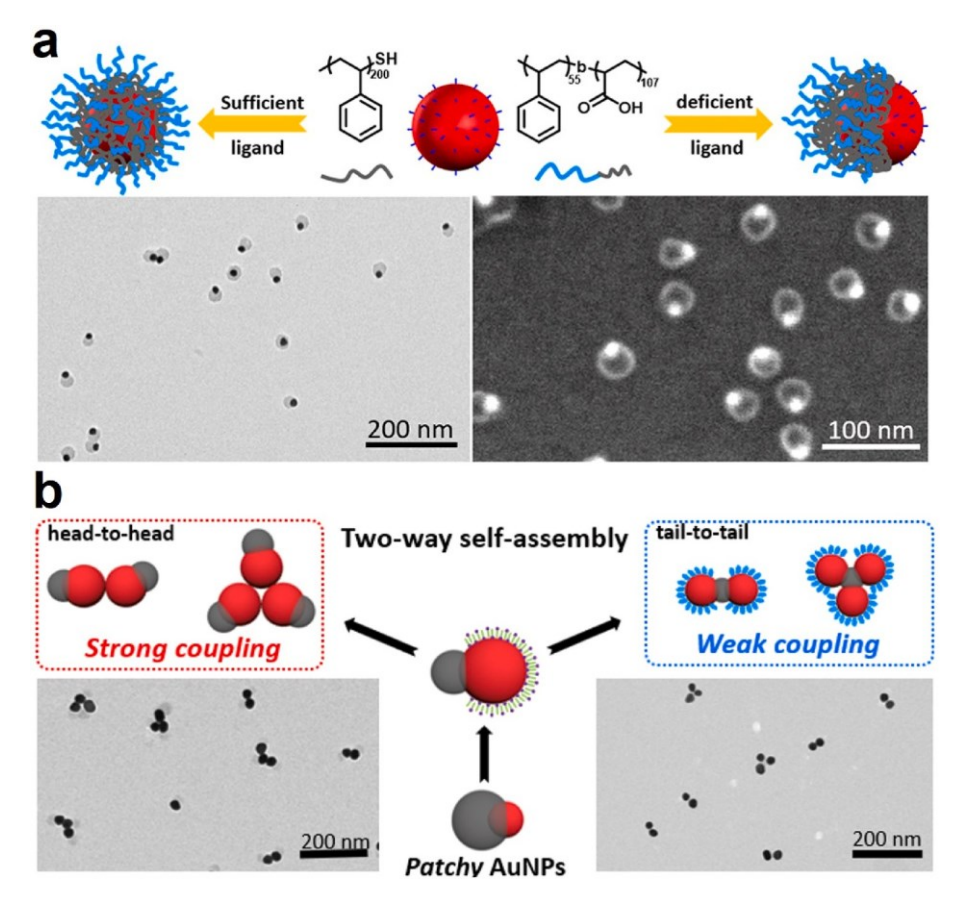


Fig. 7. (a) Schemes showing the preparation of Janus type patchy AuNPs and their corresponding TEM and SEM image. Adapted with permission from Ref. [35]. Copyright 2021 American Chemical Society. (b) Schemes showing the two-way self-assembly of grown Janus AuNPs and the corresponding TEM images of assemblies. Adapted with permission from Ref. [36]. Copyright 2022 Royal Society of Chemistry.

precisely control the polymer surface coverage of AuNPs. As guided by polymer domain, Janus-type patchy AuNPs could self-assemble in two different directions, namely head-to-head (H - H, along exposed metal surface) and tail-to-tail (T-T, along the covered surface by polymer micelles) (Fig. 7b). In the head-to-head mode, the van der Waals interaction of the exposed Au surface was used to achieve the close contact of Au cores. This generated strong interparticle plasmon coupling since less ligands existed in between AuNPs. Hydrophobicity-driven self-assembly was applied in the T-T mode where CTAB was replaced by thiol-terminated poly (ethylene oxide) (PEO-SH) and BCPs were washed away by DMF. The resulting PS-AuNP-PEO (in DMF) had mixed polymer brushes of PS-SH and PEO-SH distributed on different sides of AuNPs. As an analogue of molecular amphiphiles, those NPs could assemble into clusters along the PS-covered surface in water. The obtained clusters had a newly formed polymer domain composed of original PS ligands between patchy AuNPs, which led to relatively weak plasmon coupling. The H - H and T-T assembly products could be tuned by the size of grown AuNPs, and the underlined mechanism was the balance of interparticle interaction that can be tuned by the surface coverage.

We further extended the ligand deficiency exchange method to achieve site-specific polymer grafting on AuNRs [38]. The typical synthesis was carried out in the mixture of DMF and water containing PS_{169} -SH as polymer ligand and PS_{40} -b- PEO_{114} as a BCP surfactant. Morphological transitions were observed with varying the concentrations of PS₁₆₉-SH and water (Fig. 8a). At a high concentration of PS₁₆₉-SH, core-shell structures where AuNRs were fully covered by polymer shells were formed; while at low concentration of PS₁₆₉-SH or high water content (>9 vol%), high-purity dumbbell-like AuNRs with two polymer domains capped at each end were synthesized, exceeding 94 % purity. The critical ligand density was found to be ca. 0.08 chains/nm². Interestingly, dumbbell-like AuNRs could further polymerize into plasmonic chains at a water content of 9 vol% within 2 min when annealing at 90 °C (Fig. 8b). To understand the mechanism of chain formation, a time-dependent study of supracolloidal polymerization was conducted using UV - vis spectroscopy and TEM. Upon

annealing at 90 °C, a significant red shift in the LSPR peak indicated the end-to-end polymerization of these dumbbell-like AuNRs into chains. TEM characterization confirmed the growths of nanorod chains at different annealing periods. The kinetics of this transition were found to be strongly temperature- and solvent-dependent (Fig. 8d). A higher temperature and a lower water content accelerated the transition from dumbbell-like AuNRs to nanorod chains, while a higher water content and a lower temperature slowed down the transition (Fig. 8c and d). The activation step was attributed to the deprotection of dumbbell-like AuNRs by removing BCP, highlighting the crucial role of temperature and solvent in governing the solubility change of PS domains. In addition, site-specific polymer grafting on AuNRs could also be achieved by controlling the binding strength of polymer ligands to AuNRs at different crystalline facets [25,49,67], oxidative elimination with selective removal of polymer ligands [66], and solvent quality-mediated ligand exchange [68]. Murphy's group demonstrated that disulfide containing PEO-S-S-PEO would replace CTAB selectively at the two ends of AuNRs, while, thiol-terminated PEO (PEO-SH) replaced CTAB on the entire surface of AuNRs [49]. In a similar study, Zhu et al. demonstrated a solvent quality-mediated strategy to control regio-selective modification of AuNRs where PEO-SH would selectively go to the tips in a poor solvent of CTAB [68]. Such regioselectivity was attributed to a lower mobility of CTAB on the side of AuNRs. Furthermore, site-specific polymer grafting could also result from oxidative elimination strategy where the selective detachment of polymer ligands was seen through the oxidation etching of surface atoms at the two ends of AuNRs as reported by Liu's group [66].

The self-assembly of patchy NPs could be highly directional due to their structural anisotropy induced by polymer ligands. However, such self-assembly behaviour usually produces uncontrollable structures in terms of their equilibrium dimensions. An important feature in molecular bonding is self-limiting and self-sorting where the bond only forms between interacting atoms at a specific bonding number. PGNPs with various polymer ligands do not show regioselective self-sorting assembly, owing to lack of quantitively self-limiting interparticle interaction.

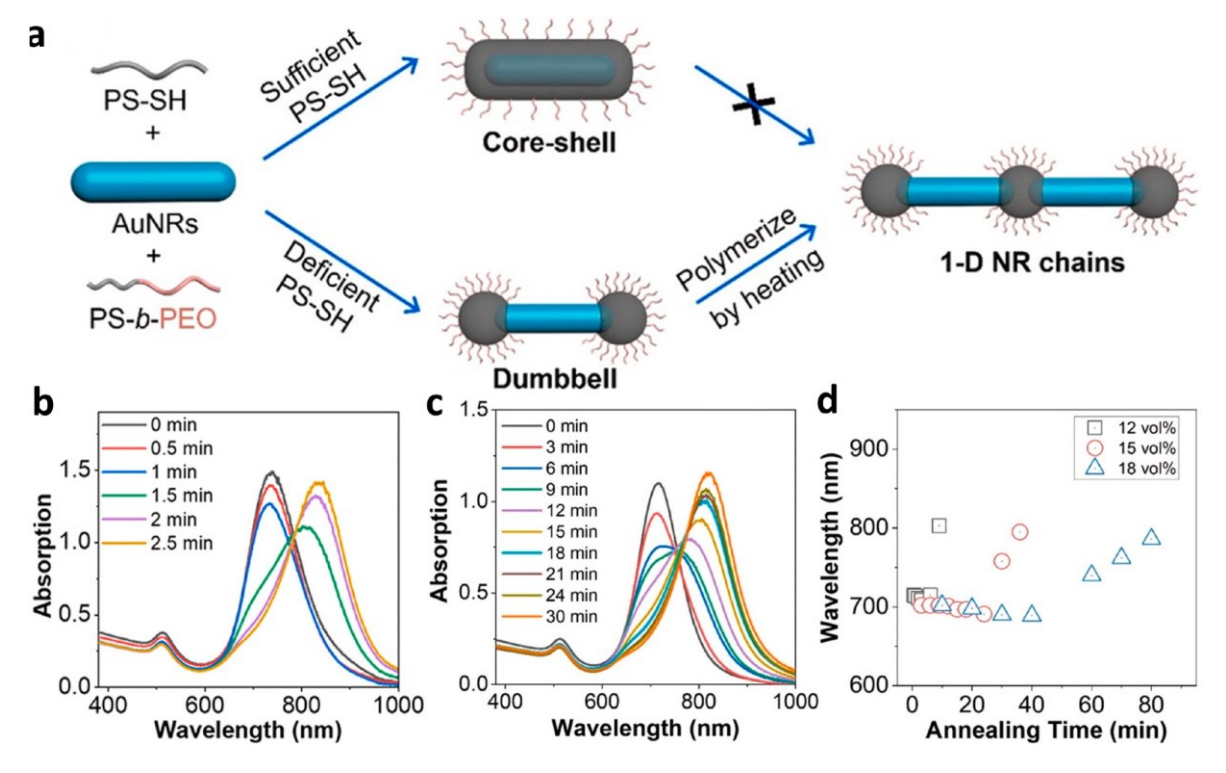


Fig. 8. (a) Schemes showing the preparation of core-shell, dumbbell-like and 1-D chain patchy AuNRs. (b - c) UV - vis absorption spectra of patchy AuNRs (9 vol% H_2O) during thermal annealing at 90 °C (b) and 80 °C (c) at different times. (d) Plotting the longitudinal plasmon band of patchy AuNRs at different water content against thermal annealing time 100 °C. Adapted with permission from Ref. [38]. Copyright 2023 American Chemical Society.

One possible solution to address their molecule-mimicking self-assembly is to introduce the complementary interactions to those building blocks through ligand engineering of polymers. Nie and co-workers reported the controlled self-assembly of isotropic NPs through charge interaction [69]. The strategy is based on the utilization of electrostatic interactions between oppositely charged particles. They first demonstrated the periodically alternating co-assembly of PGNPs with different sizes as a colloidal analogy of polymer synthesized from condensation such as Nylon-66. Two BCP ligands with negative or positive charges were synthesized as PS-b-poly (acrylic acid-r-styrene)-SH (S_x ($A_a S_{1-a}$)_v) or PS-b-poly (N,N-dimethylaminoethyl methacrylate-r-styrene)-SH (S_m $(D_{\,\beta}\,S_{1\,{\text{-}}\,\beta})_n),$ respectively. When grafting those ligands to NPs, the PS block served as buffering layer to provide colloidal stabilization in organic solvents and the other block containing randomly polymerized ionic monomers as acid or basic groups would produce directional attractions due to opposite charges. Simple mixing of NPs with those two ligands in THF in the presence of acetic acid would lead to the formation of 1-D nanochains with 100 % alternating sequence. Such a self-sorting assembly process is dominated by the charge interaction-induced oligomerization and diffusion-controlled polymerization. Later, they further developed the atom-bonding mimicking strategy, as a self-limiting process, to assemble NPs in a way like constructing molecules from atoms [5]. NPs with different sizes were functionalized with thiol-terminated PEO-b-poly (acrylic acid-r-styrene) [PEO-b-P (AA-r-St)] and PEO-poly (N,N-dimethylaminoethyl methacrylate-r-styrene) [PEO-b-P (DMAEMA-r-St)], denoted as the NP-A and NP-B, respectively. By mixing NP-A and NP-B in THF, electrostatic attraction between polymer ligands with opposite charges drove the formation of colloidal bonding of AB_x (x = 1, 2, 3, 4, 5 and 6) that mimicked the molecular bonding of two atoms. The ratio x determined by the total amount of acid and base groups (NA and NB) could be adjusted by stoichiometric control of NP-A/NP-B, grafting density, acid/base fraction in ligand and NP size. Importantly, the assembly of NP-A and NP-B is self-limited, which means that there would be no colloidal binding after the neutralization of A-B was done. Such self-limiting binding formation feature underlies the atom-bonding mimicking strategy to form colloidal clusters with a defined number of "bonding".

4. Summary and outlook

In summary, we reviewed recent advances in designing hybrid nanostructures through the combination of synthetic polymers and plasmonic NPs. We categorize two strategies based on how NPs interact with polymers: direct encapsulation and chemical grafting. In direct encapsulation, NPs with hydrophobic ligands are physically enclosed within polymer micelles, primarily through hydrophobic interactions. We discussed strategies for controlling the loading numbers and locations of NPs within polymer micelles. When using a single type of hydrophobic ligand on NPs, direct encapsulation typically results in symmetric polymer coatings on NPs. The hydrophobicity-driven co-selfassembly of NPs and amphiphilic BCPs is often kinetically controlled to yield NP clusters with different numbers of NPs, requiring densitygradient centrifugation to separate clusters with precise numbers of NPs. When using binary or mixed hydrophobic/hydrophilic ligands, the location of NPs and their clusters in polymer micelles can be controlled to be either concentric or eccentric, depending on the balance of their surface ligand species. Alternatively, polymer ligands can asymmetrically coat metal NPs through hydrophobicity-driven phase segregation. We highlight the asymmetric surface patterning of metal NPs using homopolymers, BCPs, and blocky random copolymers. Symmetry breaking is of key importance in colloidal synthesis and self-assembly to generate anisotropic interparticle interactions and guide the selfassembly of colloidal NPs. By selectively patching polymer ligands on the surface of NPs, these ligands provide directional interactions that drive the self-assembly of NPs. The use of complementary interactions on polymer ligands can further provide self-limiting interactions among

NPs, controlling colloidal clustering to mimic atomic bonding.

There has been tremendous progress in designing new hybrid nanostructures of polymers with plasmonic NPs. Several remaining challenges will require ongoing efforts in this field. First of all, the customizable design of synthetic polymers and plasmonic NPs remains a significant challenge. Although there have been advancements in understanding the surface engineering of plasmonic NPs, particularly in asymmetric surface patterning using hydrophobic polymers, precise control over these ligands in terms of domain sizes, numbers, and chemical functionalities on NP surfaces is still in its early stages. For instance, isotropic AuNPs grafted by hydrophobic PS ligands can potentially have multiple polymer domains upon the change of solvent quality, if the size of AuNPs is much larger than the end-to-end distance of PS. These polymer domains often exhibit ill-defined sizes and random distributions on AuNPs [63]. The use of these patched NPs as building blocks for self-assembly is, therefore, limited by their unpredictable synthesis. With the rapid evolution of their surface chemistry, new synthetic methods are highly desirable to achieve next-level control synthesis of polymer/NP hybrids with potentially customizable nanostructures. Secondly, the length scale of polymers offers advantages for the colloidal stability of grafted NPs and for guiding their self-assembly. Yet, this length scale is also at the limit of strong plasmon coupling. For instance, polymers used as surface ligands bind to metal NPs in an extended brush-like conformation. These brush-like chains create large interparticle distances, even in a poor solvent, that significantly weakens the plasmon coupling of metal NPs. The conformation of polymer chains is a crucial parameter for controlling the optical properties of plasmon NP assemblies, but it has not been extensively studied before. Our group recently demonstrated that multidentate but weak binding motifs, like COOH in poly (acrylic acid), can bind to metal NPs through surface wrapping [70]. These multidentate polymer ligands can significantly decrease interparticle distances in NP aggregates, enhancing interparticle plasmon coupling. Lastly, most studies on hybrid nanostructures of polymers and plasmonic NPs have predominantly focused on precious metals like Au and Ag. While these metals are chemically stable and easily prepared through wet-chemical synthesis, they are not cost-effective. Plasmonic NPs containing Cu, for example, have not been explored in terms of their polymer encapsulation or surface grafting. Importantly, the LSPR bands of precious metals are limited to the visible and infrared range. For biological applications of hybrid polymers and plasmonic NPs, such as surface-enhanced Raman scattering (SERS) of biomacromolecules, the resonance peaks of proteins and DNA are at 250 - 300 nm [71]. Other metal NPs, like aluminum, have a broader LSPR that could bring new excitement to use the hybrid nanostructures of polymers with plasmonic NPs [72 - 74].

CRediT authorship contribution statement

Hanyi Duan: Writing - review & editing, Writing - original draft.

Debasmita Muhuri: Writing - review & editing, Writing - original draft.

Jie He: Writing - review & editing, Writing - original draft.

Declaration of competing interest

The authors declare the following financial interests/personal relationships which may be considered as potential competing interests:

Jie He reports financial support was provided by National Science Foundation. If there are other authors, they declare that they have no known competing financial interests or personal relationships that could have appeared to influence the work reported in this paper.

Data availability

The authors do not have permission to share data.

Acknowledgements

The authors thank for the financial support from the National Science Foundation (CHE 2102245).

References

- [1] Y. Sun, Y. Xia, Shape-controlled synthesis of gold and silver nanoparticles, Science 298 (5601) (2002) 2176 - 2179.
- M. Grzelczak, J. P'erez-Juste, P. Mulvaney, L.M. Liz-Marza'n, Shape control in gold
- nanoparticle synthesis, Chem. Soc. Rev. 37 (9) (2008) 1783 [–] 1791. [3] T.H. Yang, Y. Shi, A. Janssen, Y. Xia, Surface capping agents and their roles in shape-controlled synthesis of colloidal metal nanocrystals, Angew. Chem. Int. Ed. 59 (36) (2020) 15378 - 15401.
- [4] J. P'erez-Juste, I. Pastoriza-Santos, L.M. Liz-Marz'an, P. Mulvaney, Gold nanorods: synthesis, characterization and applications, Coord. Chem. Rev. 249 (17) (2005) 1870 - 1901.
- [5] C. Yi, H. Liu, S. Zhang, Y. Yang, Y. Zhang, Z. Lu, E. Kumacheva, Z. Nie, Self-limiting directional nanoparticle bonding governed by reaction stoichiometry, Science 369 (6509) (2020) 1369 - 1374.
- [6] P.J. Santos, P.A. Gabrys, L.Z. Zornberg, M.S. Lee, R.J. Macfarlane, Macroscopic materials assembled from nanoparticle superlattices, Nature 591 (7851) (2021)
- [7] A. Klinkova, R.M. Choueiri, E. Kumacheva, Self-assembled plasmonic nostructures, Chem. Soc. Rev. 43 (11) (2014) 3976 - 3991.
- W.A. Murray, W.L. Barnes, Plasmonic materials, Adv. Mater. 19 (22) (2007)
- [9] D. García-Lojo, S. Nún ez-Sa nchez, S. Go mez-Gran a, M. Grzelczak, I. Pastoriza-Santos, J. P'erez-Juste, L.M. Liz-Marza'n, Plasmonic supercrystals, Acc. Chem. Res. 52 (7) (2019) 1855 - 1864.
- [10] S. Oldenburg, R. Averitt, S. Westcott, N. Halas, Nanoengineering of optical esonances, Chem. Phys. Lett. 288 (2 - 4) (1998) 243 - 247.
- [11] N.J. Halas, S. Lal, W.-S. Chang, S. Link, P. Nordlander, Plasmons in strongly coupled metallic nanostructures, Chem. Rev. 111 (6) (2011) 3913 - 3961.
- [12] A.M. Funston, C. Novo, T.J. Davis, P. Mulvaney, Plasmon coupling of gold nanorods at short distances and in different geometries, Nano Lett. 9 (4) (2009)
- [13] P.K. Jain, M.A. El-Sayed, Plasmonic coupling in noble metal nanostructures, Chem. Phys. Lett. 487 (4) (2010) 153 - 164.
- [14] A. Campion, P. Kambhampati, Surface-enhanced Raman scattering, Chem. Soc. Rev. 27 (4) (1998) 241 - 250.
- [15] S.K. Ghosh, T. Pal, Interparticle coupling effect on the surface plasmon resonance of gold nanoparticles: from theory to applications, Chem. Rev. 107 (11) (2007)
- [16] P.L. Stiles, J.A. Dieringer, N.C. Shah, R.P. Van Duyne, Surface-enhanced Raman spectroscopy, Annu. Rev. Anal. Chem. 1 (2008) 601 – 626.

 [17] S. Schlücker, Surface-Enhanced Raman spectroscopy: concepts and chemical
- applications, Angew. Chem. Int. Ed. 53 (19) (2014) 4756 4795.
- [18] B. Sharma, R.R. Frontiera, A.-I. Henry, E. Ringe, R.P. Van Duyne, SERS: materials, applications, and the future, Mater. Today 15 (1) (2012) 16 - 25.
- [19] J. Langer, D. Jimenez de Aberasturi, J. Aizpurua, R.A. Alvarez-Puebla, B. Augui e, J. J. Baumberg, G.C. Bazan, S.E.J. Bell, A. Boisen, A.G. Brolo, J. Choo, D. Cialla-May, V. Deckert, L. Fabris, K. Faulds, F.J. García de Abajo, R. Goodacre, D. Graham, A. J. Haes, C.L. Haynes, C. Huck, T. Itoh, M. Ka"ll, J. Kneipp, N.A. Kotov, H. Kuang, E. C. Le Ru, H.K. Lee, J.-F. Li, X.Y. Ling, S.A. Maier, T. Mayerho" fer, M. Moskovits, K. Murakoshi, J.-M. Nam, S. Nie, Y. Ozaki, I. Pastoriza-Santos, J. Perez-Juste, J. Popp, A. Pucci, S. Reich, B. Ren, G.C. Schatz, T. Shegai, S. Schlücker, L.-L. Tay, K. G. Thomas, Z.-Q. Tian, R.P. Van Duyne, T. Vo-Dinh, Y. Wang, K.A. Willets, C. Xu, H. Xu, Y. Xu, Y.S. Yamamoto, B. Zhao, L.M. Liz-Marza'n, Present and future of surface-enhanced Raman scattering, ACS Nano 14 (1) (2020) 28 - 117.
- [20] B. Sepúlveda, P.C. Angelom'e, L.M. Lechuga, L.M. Liz-Marza'n, LSPR-based nobiosensors, Nano Today 4 (3) (2009) 244 - 251.
- [21] H. Duan, Y. Yang, Y. Zhang, C. Yi, Z. Nie, J. He, What is next in polymer-grafted plasmonic nanoparticles? Giant 4 (2020) 100033.
- C. Yi, Y. Yang, B. Liu, J. He, Z. Nie, Polymer-guided assembly of inorganic [22] nanoparticles, Chem. Soc. Rev. 49 (2) (2020) 465 - 508.
- [23] C.A. Mirkin, R.L. Letsinger, R.C. Mucic, J.J. Storhoff, A DNA-based method for rationally assembling nanoparticles into macroscopic materials, Nature 382 (6592) (1996) 607 – 609.
- [24] J. Zhang, P.J. Santos, P.A. Gabrys, S. Lee, C. Liu, R.J. Macfarlane, Self-Assembling nanocomposite tectons, J. Am. Chem. Soc. 138 (50) (2016) 16228 – 16231.
 [25] Z. Nie, D. Fava, E. Kumacheva, S. Zou, G.C. Walker, M. Rubinstein, Self-assembly of
- metal polymer analogues of amphiphilic triblock copolymers, Nat. Mater. 6 (8) (2007) 609 - 614.
- [26] R.M. Choueiri, A. Klinkova, H.s. Th'erien-Aubin, M. Rubinstein, E. Kumacheva, Structural transitions in nanoparticle assemblies governed by competing nanoscale forces, J. Am. Chem. Soc. 135 (28) (2013) 10262 - 10265.
- [27] N.R. Jana, L. Gearheart, C.J. Murphy, Seeding growth for size control of 5-40 nm diameter gold nanoparticles, Langmuir 17 (22) (2001) 6782 - 6786.
- [28] C.J. Murphy, T.K. Sau, A.M. Gole, C.J. Orendorff, J. Gao, L. Gou, S.E. Hunyadi, T. Li, Anisotropic metal nanoparticles: synthesis, assembly, and optical applications, J. Phys. Chem. B 109 (29) (2005) 13857 - 13870.
- F291 S. Mourdikoudis, L.M. Liz-Marz an, Oleylamine in nanoparticle synthesis, Chem. Mater. 25 (9) (2013) 1465 - 1476.

- [30] J. Zhou, J. Ralston, R. Sedev, D.A. Beattie, Functionalized gold nanoparticles: synthesis, structure and colloid stability, J. Colloid Interface Sci. 331 (2) (2009) 251 - 262.
- [31] W. Wang, Q.-Q. Wei, J. Wang, B.-C. Wang, S.-h. Zhang, Z. Yuan, Role of thiolcontaining polyethylene glycol (thiol-PEG) in the modification process of gold nanoparticles (AuNPs): stabilizer or coagulant? J. Colloid Interface Sci. 404 (2013) 223 - 229.
- [32] Z. Zhang, H. Li, F. Zhang, Y. Wu, Z. Guo, L. Zhou, J. Li, Investigation of halideinduced aggregation of Au nanoparticles into spongelike gold, Langmuir 30 (10) (2014) 2648 - 2659.
- [33] F. Schulz, T. Vossmeyer, N.G. Bastús, H. Weller, Effect of the spacer structure on the stability of gold nanoparticles functionalized with monodentate thiolated poly (ethylene glycol) ligands, Langmuir 29 (31) (2013) 9897 - 9908.
- [34] G. Chen, Y. Wang, L.H. Tan, M. Yang, L.S. Tan, Y. Chen, H. Chen, High-purity separation of gold nanoparticle dimers and trimers, J. Am. Chem. Soc. 131 (12) (2009) 4218 - 4219.
- [35] H. Duan, Q. Luo, Z. Wei, Y. Lin, J. He, Symmetry-broken patches on gold nanoparticles through deficient ligand exchange, ACS Macro Lett. 10 (7) (2021)
- [36] H. Duan, T. Malesky, J. Wang, C.-H. Liu, H. Tan, M.-P. Nieh, Y. Lin, J. He, Patchy metal nanoparticles with polymers: controllable growth and two-way selfassembly, Nanoscale 14 (19) (2022) 7364 - 7371.
- [37] Y. Yang, C. Yi, X. Duan, Q. Wu, Y. Zhang, J. Tao, W. Dong, Z. Nie, Block-random copolymer-micellization-mediated formation of polymeric patches on gold nanoparticles, J. Am. Chem. Soc. 143 (13) (2021) 5060 - 5070.
- [38] H. Duan, Z. Jia, M. Liaqat, M.D. Mellor, H. Tan, M.-P. Nieh, Y. Lin, S. Link, C. F. Landes, J. He, Site-specific chemistry on gold nanorods: curvature-guided surface dewetting and supracolloidal polymerization, ACS Nano 17 (13) (2023) 12788 - 12797.
- [39] Y. Kang, T.A. Taton, Controlling shell thickness in core- shell gold nanoparticles ia surface-templated adsorption of block copolymer surfactants, Macromolecules 38 (14) (2005) 6115 - 6121.
- [40] Y. Kang, T.A. Taton, Core/shell gold nanoparticles by self-assembly and crosslinking of micellar, block-copolymer shells, Angew. Chem. Int. Ed. 44 (3) (2005) 409 - 412.
- [41] A. S'anchez-Iglesias, M. Grzelczak, T. Altantzis, B. Goris, J. P'erez-Juste, S. Bals, G. Van Tendeloo, S.H. Donaldson, B.F. Chmelka, J.N. Israelachvili, L.M. Liz-Marz'an, Hydrophobic interactions modulate self-assembly of nanoparticles, ACS Nano 6 (12) (2012) 11059 - 11065.
- [42] G. Chen, Y. Wang, M. Yang, J. Xu, S.J. Goh, M. Pan, H. Chen, Measuring ensembleaveraged surface-enhanced Raman scattering in the hotspots of colloidal nanoparticle dimers and trimers, J. Am. Chem. Soc. 132 (11) (2010) 3644 - 3645.
- [43] A.S. Urban, X. Shen, Y. Wang, N. Large, H. Wang, M.W. Knight, P. Nordlander, H. Chen, N.J. Halas, Three-dimensional plasmonic nanoclusters, Nano Lett. 13 (9) (2013) 4399 - 4403.
- Y. Wang, G. Chen, M. Yang, G. Silber, S. Xing, L.H. Tan, F. Wang, Y. Feng, X. Liu, S. Li, H. Chen, A systems approach towards the stoichiometry-controlled heterosembly of nanoparticles, Nat. Commun. 1 (1) (2010) 87.
- [45] Q. Luo, R.J. Hickey, S.-J. Park, Controlling the location of nanoparticles in colloidal ssemblies of amphiphilic polymers by tuning nanoparticle surface chemistry, ACS Macro Lett. 2 (2) (2013) 107 - 111.
- [46] R.J. Hickey, Q. Luo, S.-J. Park, Polymersomes and multicompartment polymersomes formed by the interfacial self-assembly of gold nanoparticles and amphiphilic polymers, ACS Macro Lett. 2 (9) (2013) 805 - 808.
- [47] T. Chen, M. Yang, X. Wang, L.H. Tan, H. Chen, Controlled assembly of eccentrically encapsulated gold nanoparticles, J. Am. Chem. Soc. 130 (36) (2008) 11858 - 11859.
- [48] A. Kim, S. Zhou, L. Yao, S. Ni, B. Luo, C.E. Sing, Q. Chen, Tip-patched nanoprisms from formation of ligand islands, J. Am. Chem. Soc. 141 (30) (2019) 11796 - 11800.
- [49] J.G. Hinman, J.R. Eller, W. Lin, J. Li, J. Li, C.J. Murphy, Oxidation state of capping agent affects spatial reactivity on gold nanorods, J. Am. Chem. Soc. 139 (29) (2017) 9851 - 9854.
- Y. Liu, M. Klement, Y. Wang, Y. Zhong, B. Zhu, J. Chen, M. Engel, X. Ye, Macromolecular ligand engineering for programmable nanoprism assembly, J. Am. Chem. Soc. 143 (39) (2021) 16163 - 16172.
- [51] K. Liu, Z. Nie, N. Zhao, W. Li, M. Rubinstein, E. Kumacheva, Step-growth polymerization of inorganic nanoparticles, Science 329 (5988) (2010) 197 - 200.
- [52] A. Kim, T. Vo, H. An, P. Banerjee, L. Yao, S. Zhou, C. Kim, D.J. Milliron, S. C. Glotzer, Q. Chen, Symmetry-breaking in patch formation on triangular gold nanoparticles by asymmetric polymer grafting, Nat. Commun. 13 (1) (2022) 1 - 14.
- [53] J. Zhou, M.N. Creyer, A. Chen, W. Yim, R.P.M. Lafleur, T. He, Z. Lin, M. Xu, P. Abbasi, J. Wu, T.A. Pascal, F. Caruso, J.V. Jokerst, Stereoselective growth of small molecule patches on nanoparticles, J. Am. Chem. Soc. 143 (31) (2021) 12138 - 12144.
- [54] L. Zhang, Z. Wei, S. Thanneeru, M. Meng, M. Kruzyk, G. Ung, B. Liu, J. He, A polymer solution to prevent nanoclustering and improve the selectivity of metal nanoparticles for electrocatalytic CO2 reduction, Angew. Chem. Int. Ed. 131 (44) (2019) 15981 - 15987.
- [55] S. Thanneeru, K.M. Ayers, M. Anuganti, L. Zhang, C.V. Kumar, G. Ung, J. He, N-Heterocyclic carbene-ended polymers as surface ligands of plasmonic metal nanoparticles, J. Mater. Chem. C 8 (7) (2020) 2280 - 2288.
- [56] D. Julthongpiput, Y.-H. Lin, J. Teng, E.R. Zubarev, V.V. Tsukruk, Y-shaped amphiphilic brushes with switchable micellar surface structures, J. Am. Chem. Soc. 125 (51) (2003) 15912 - 15921.
- [57] J. He, Y. Liu, T. Babu, Z. Wei, Z. Nie, Self-assembly of inorganic nanoparticle vesicles and tubules driven by tethered linear block copolymers, J. Am. Chem. Soc. 134 (28) (2012) 11342 - 11345.

- [58] J. He, X. Huang, Y.-C. Li, Y. Liu, T. Babu, M.A. Aronova, S. Wang, Z. Lu, X. Chen, Z. Nie, Self-assembly of amphiphilic plasmonic micelle-like nanoparticles in selective solvents, J. Am. Chem. Soc. 135 (21) (2013) 7974 – 7984.
- [59] J. Song, L. Cheng, A. Liu, J. Yin, M. Kuang, H. Duan, Plasmonic vesicles of amphiphilic gold nanocrystals: self-assembly and external-stimuli-triggered destruction, J. Am. Chem. Soc. 133 (28) (2011) 10760 – 10763.
- [60] W. Li, S. Liu, R. Deng, J. Zhu, Encapsulation of nanoparticles in block copolymer micellar aggregates by directed supramolecular assembly, Angew. Chem. Int. Ed. 50 (26) (2011) 5865 – 5868.
- [61] K. Wang, S.-M. Jin, F. Li, D. Tian, J. Xu, E. Lee, J. Zhu, Soft confined assembly of polymer-tethered inorganic nanoparticles in cylindrical micelles, Macromolecules 53 (12) (2020) 4925 – 4931.
- [62] H. Duan, Y. Lin, J. He, Metal nanoparticles grafted with polymeric ligands: self-assembly guided by polymers in solution, in: Y. Yin, Y. Lu, Y. Xia (Eds.), Encyclopedia of Nanomaterials, first ed., Elsevier, Oxford, 2023, pp. 390 – 406.
- [63] R.M. Choueiri, E. Galati, H. Th´erien-Aubin, A. Klinkova, E.M. Larin, A. Querejeta-Ferna´ındez, L. Han, H.L. Xin, O. Gang, E.B. Zhulina, M. Rubinstein, E. Kumacheva, Surface patterning of nanoparticles with polymer patches, Nature 538 (7623) (2016) 79 83.
- [64] B. Liu, S. Thanneeru, A. Lopes, L. Jin, M. McCabe, J. He, Surface engineering of spherical metal nanoparticles with polymers toward selective asymmetric synthesis of nanobowls and janus-type dimers, Small 13 (20) (2017) 1700091.
- [65] C. Rossner, E.B. Zhulina, E. Kumacheva, Staged surface patterning and self-assembly of nanoparticles functionalized with end-grafted block copolymer ligands, Angew. Chem. Int. Ed. 58 (27) (2019) 9269 9274.
- [66] J. Kang, Y.-X. Wang, F. Peng, N.-N. Zhang, Y. Xue, Y. Yang, E. Kumacheva, K. Liu, Oxidative elimination and reductive addition of thiol-terminated polymer ligands to metal nanoparticles, Angew. Chem. Int. Ed. 61 (35) (2022) e202202405.
- [67] F. Wang, S. Cheng, Z. Bao, J. Wang, Anisotropic overgrowth of metal heterostructures induced by a site-selective silica coating, Angew. Chem. Int. Ed. 52 (39) (2013) 10344 – 10348.
- [68] F. Li, K. Wang, Z. Tan, C. Guo, Y. Liu, H. Tan, L. Zhang, J. Zhu, Solvent quality-mediated regioselective modification of gold nanorods with thiol-terminated polymers, Langmuir 36 (49) (2020) 15162 15168.
- [69] C. Yi, Y. Yang, Z. Nie, Alternating copolymerization of inorganic nanoparticles, J. Am. Chem. Soc. 141 (19) (2019) 7917 – 7925.
- [70] Z. Wei, A. Vandergriff, C.-H. Liu, M. Liaqat, M.-P. Nieh, Y. Lei, J. He, Strongly coupled plasmonic metal nanoparticles with reversible pH-responsiveness and highly reproducible SERS in solution, Nanoscale 16 (2) (2024) 708 718.
- [71] A. Dubey, R. Mishra, C.-W. Cheng, Y.-P. Kuang, S. Gwo, T.-J. Yen, Demonstration of a superior deep-UV surface-enhanced resonance Raman scattering (SERRS) substrate and single-base mutation detection in oligonucleotides, J. Am. Chem. Soc. 143 (46) (2021) 19282 – 19286.
- [72] S. Tian, O. Neumann, M.J. McClain, X. Yang, L. Zhou, C. Zhang, P. Nordlander, N. J. Halas, Aluminum nanocrystals: a sustainable substrate for quantitative SERS-based DNA detection, Nano Lett. 17 (8) (2017) 5071 5077.
- [73] S. Lu, H. Yu, S. Gottheim, H. Gao, C.J. DeSantis, B.D. Clark, J. Yang, C.R. Jacobson, Z. Lu, P. Nordlander, Polymer-Directed growth of plasmonic aluminum nanocrystals, J. Am. Chem. Soc. 140 (45) (2018) 15412 – 15418.
- [74] F. Peng, S.-Y. Lu, P.-Q. Sun, N.-N. Zhang, K. Liu, Branched aluminum nanocrystals with internal hot spots: synthesis and single-particle surface-enhanced Raman scattering, Nano Lett. 23 (14) (2023) 6567 – 6573.



Hanyi Duan obtained his B.S. in Taiyuan University of Technology in 2015. Then he moved to Zhejiang University and got his M.S. in 2018 under the supervision of Prof. Xinghong Zhang. He is a PhD student in Prof. Jie He's lab from 2019 to 2024. His research mainly focuses on the preparation and self-assembly of patchy nanoparticles.



Debasmita Muhuri received her B.Sc. (2020) and M.Sc. (2022) both from Jadavpur University, Kolkata, West Bengal, India under the supervision of Dr. Partha Roy. Then she worked on a project in Indian Institute of Science Education and Research (IISER) Kolkata, India under supervision of Dr. Debansu Chaudhuri in 2022. Now she has joined Dr. Jie He's research group in the University of Connecticut in fall 2023. Her research is mainly focused on the surface chemistry of noble metal nanoparticles.



Jie He earned his B.S. and M.S. degrees in Polymer Materials Science and Engineering from Sichuan University and his Ph.D. in Chemistry with Prof. Yue Zhao from the Universit'e de Sherbrooke in 2010. After working with Professor Zhihong Nie as a postdoctoral fellow at the University of Maryland, he joined the faculty of the University of Connecticut where he is currently a Professor of Chemistry and Polymer Program. His group focuses on the design of hybrid materials of polymers and inorganic materials (metal ions, clusters, and nanoparticles) being capable of catalyzing the activation of small molecules as inspired by nature.